Electronic Supplementary Material (ESI) for Dalton Transactions

Coordination self-assembly of tetranuclear Pt(II) macrocycles with organometallic backbone for sensing of acyclic dicarboxylic acids

Sankarasekaran Shanmugaraju,[a] Arun Kumar Bar,[a] Harshal Jadhav,[a] Dohyun Moon,*[b] and Partha Sarathi Mukherjee*[a]

[a]*Department of Inorganic and Physical Chemistry, Indian Institute of Science, Bangalore-560 012, India. Fax: 91-80-2360-1552; Tel; 91-80-2293-3352*

E-mail: psm@ipc.iisc.ernet.in

[b]*Pohang Accelerator Laboratory, Pohang, Kyungbook-790784, South Korea*

E-mail: dmoon@postech.ac.kr

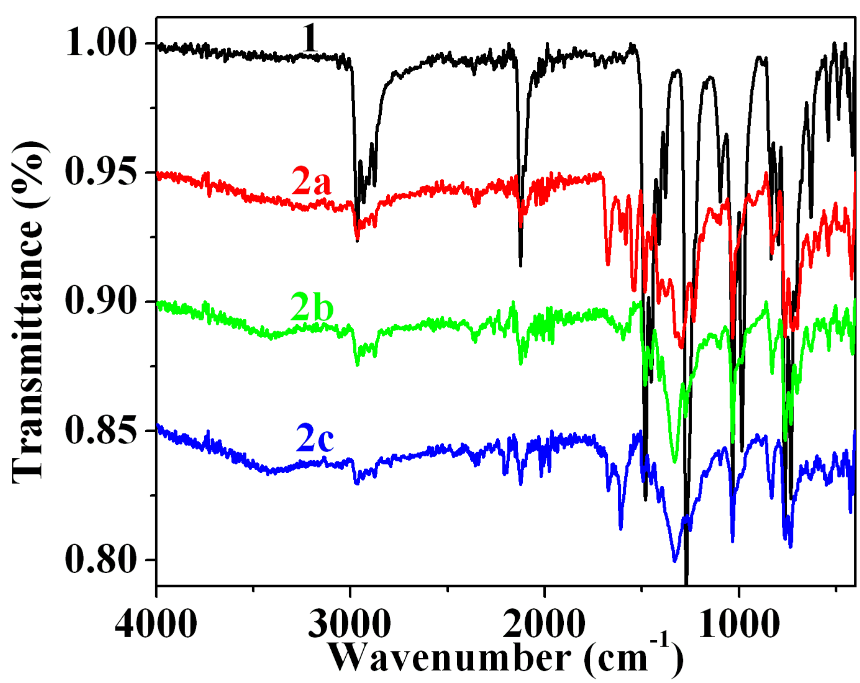

Fig. S1. IR spectra of **1**, **2a**–**2c**.

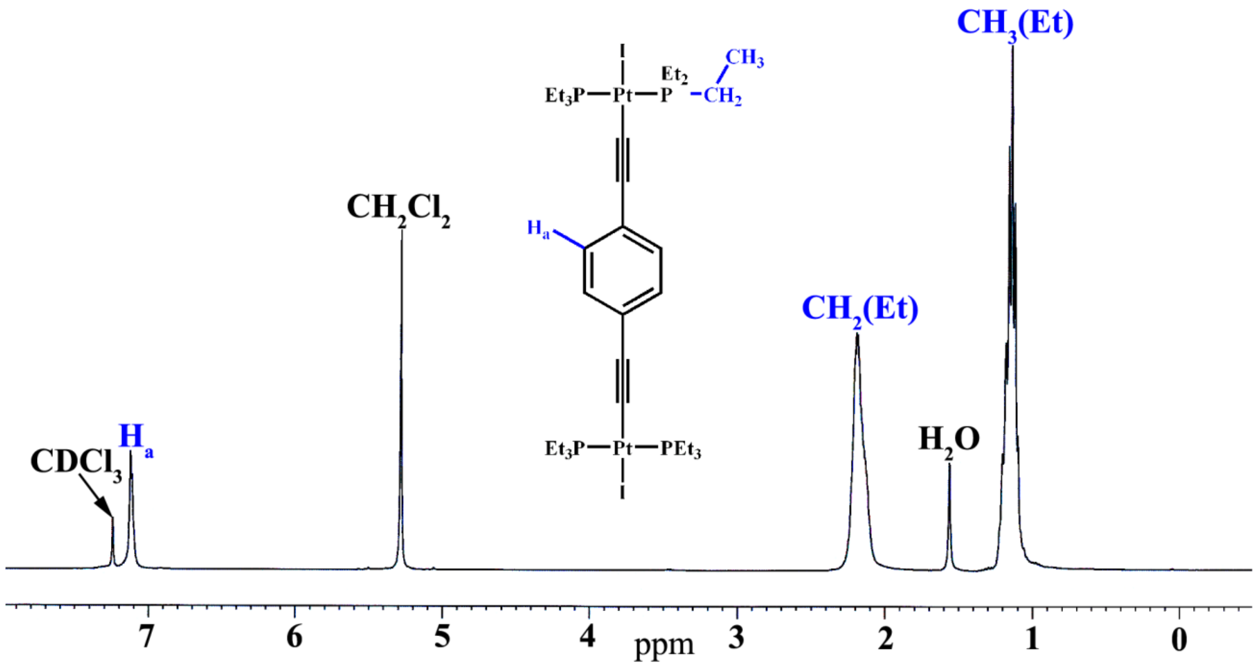

Fig. S2. [1]H NMR spectra of 1,4-bis[*trans*-Pt(PEt_3)$_2$I(ethynyl)]benzene (**1a**) recorded in $CDCl_3$ with the peak assignments.

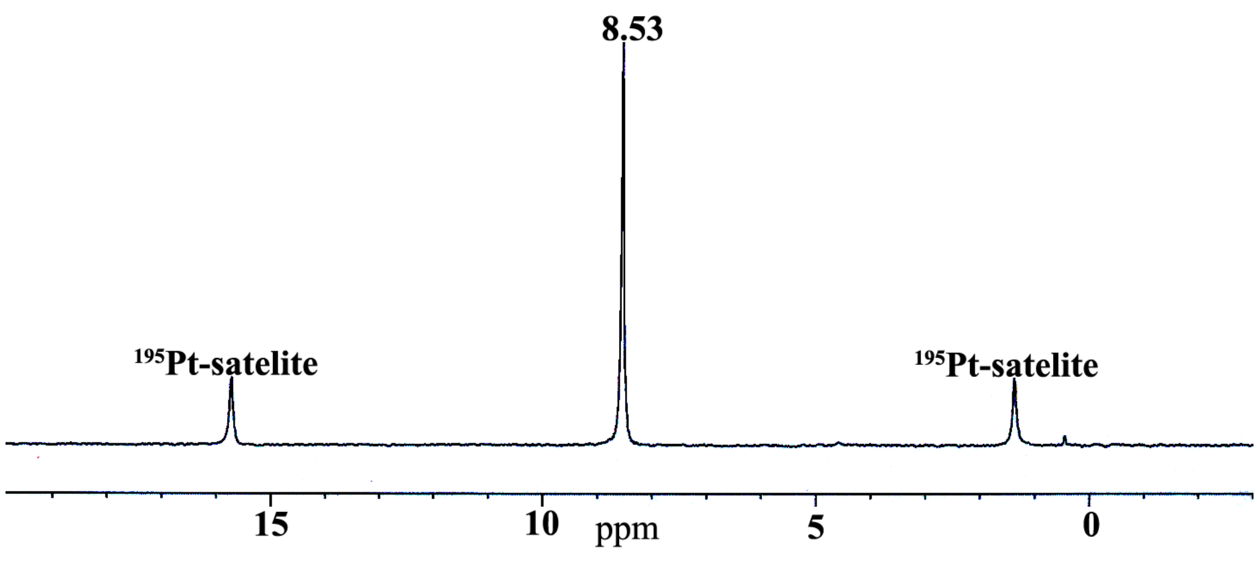

Fig. S3. [31]P NMR spectra of 1,4-bis[*trans*-Pt(PEt_3)$_2$I(ethynyl)]benzene (**1a**) recorded in $CDCl_3$.

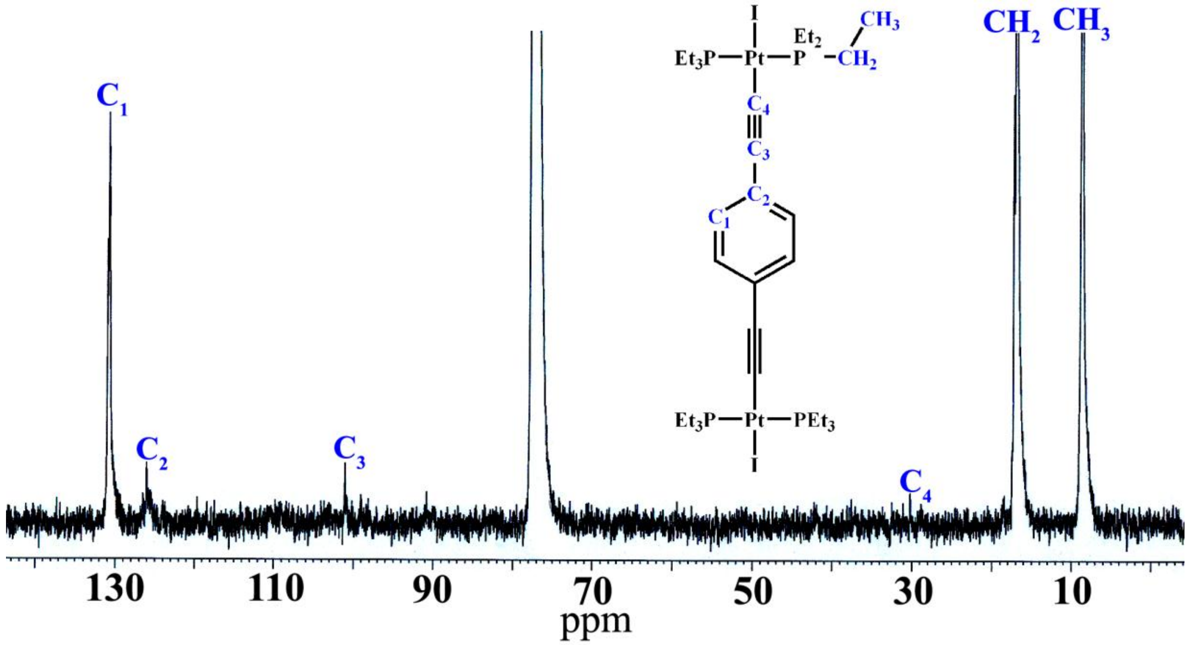

Fig. S4. ^{13}C NMR spectra of 1,4-bis[*trans*-Pt(PEt_3)$_2$I(ethynyl)]benzene (**1a**) recorded in $CDCl_3$.

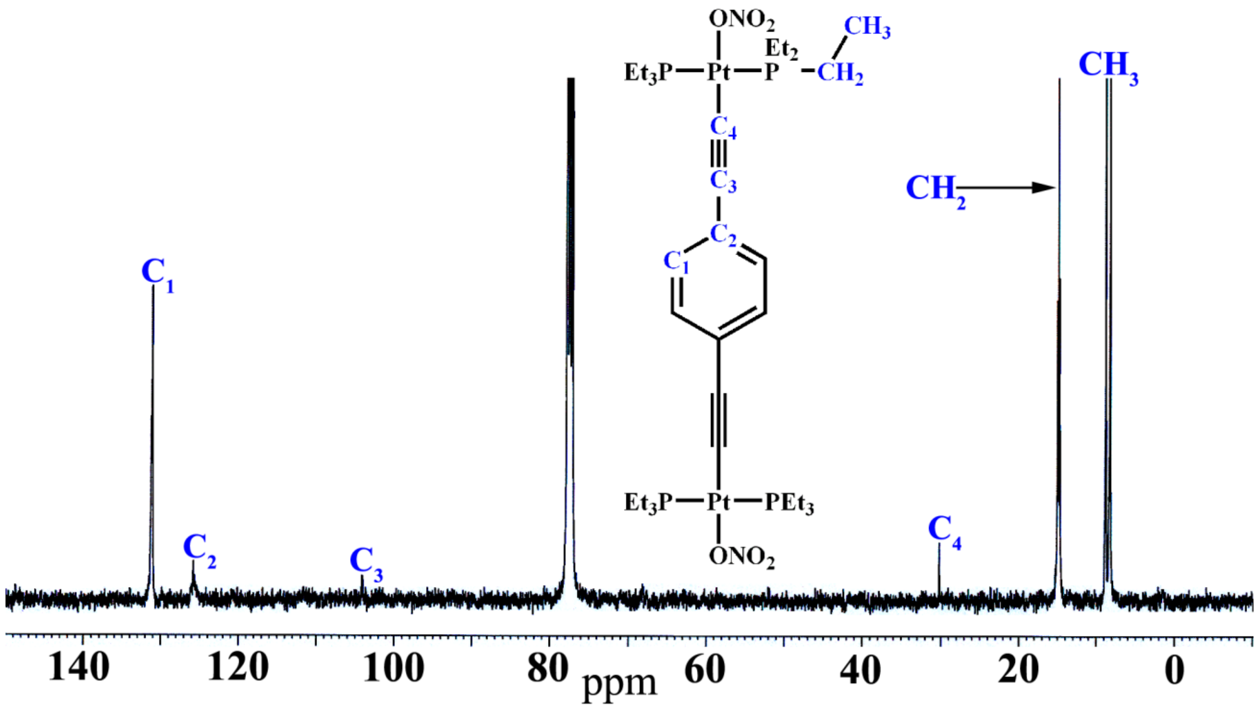

Fig. S5. ^{13}C NMR spectra of the binuclear acceptor **1** recorded in $CDCl_3$.

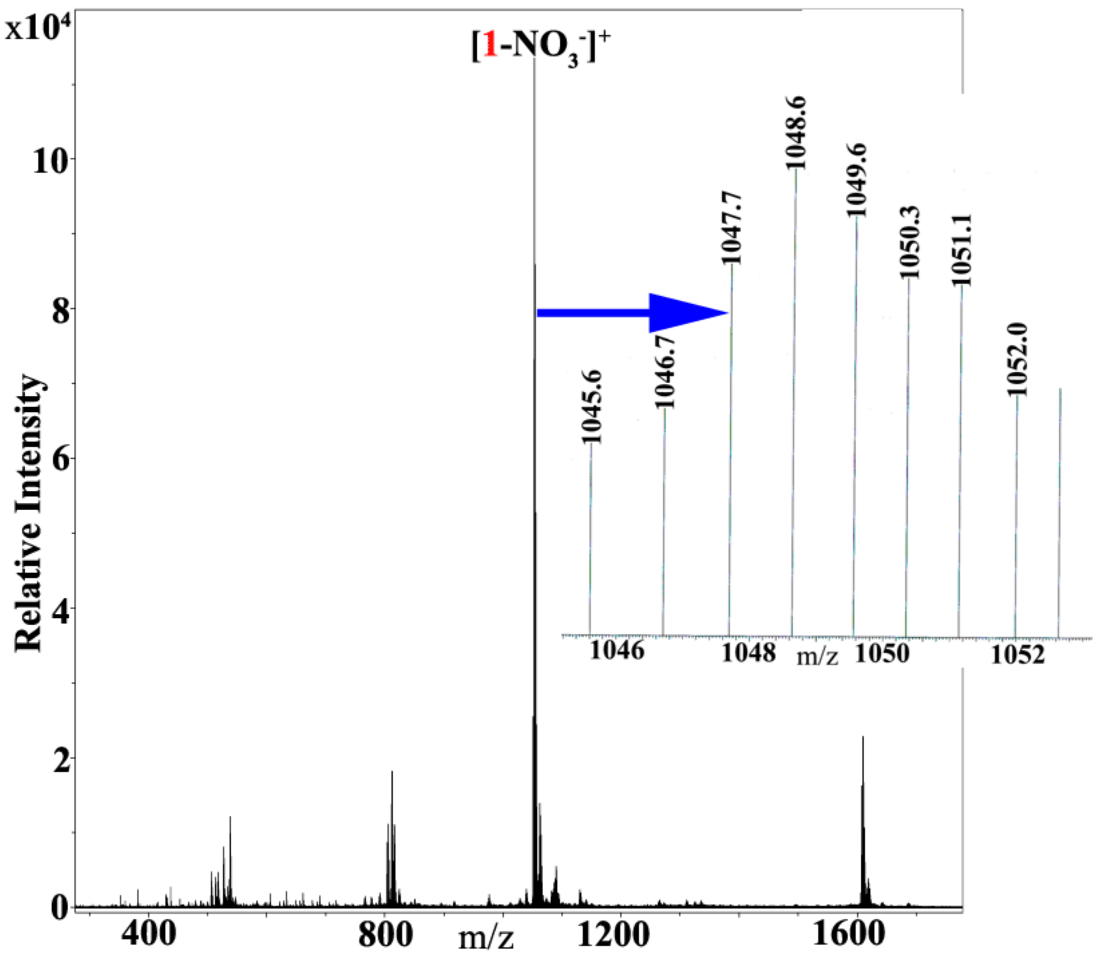

Fig. S6. ESI-MS spectrum of the acceptor **1** recorded in acetonitrile. Inlet; experimentally observed isotopic distribution for [**1** − NO_3^-]$^+$.

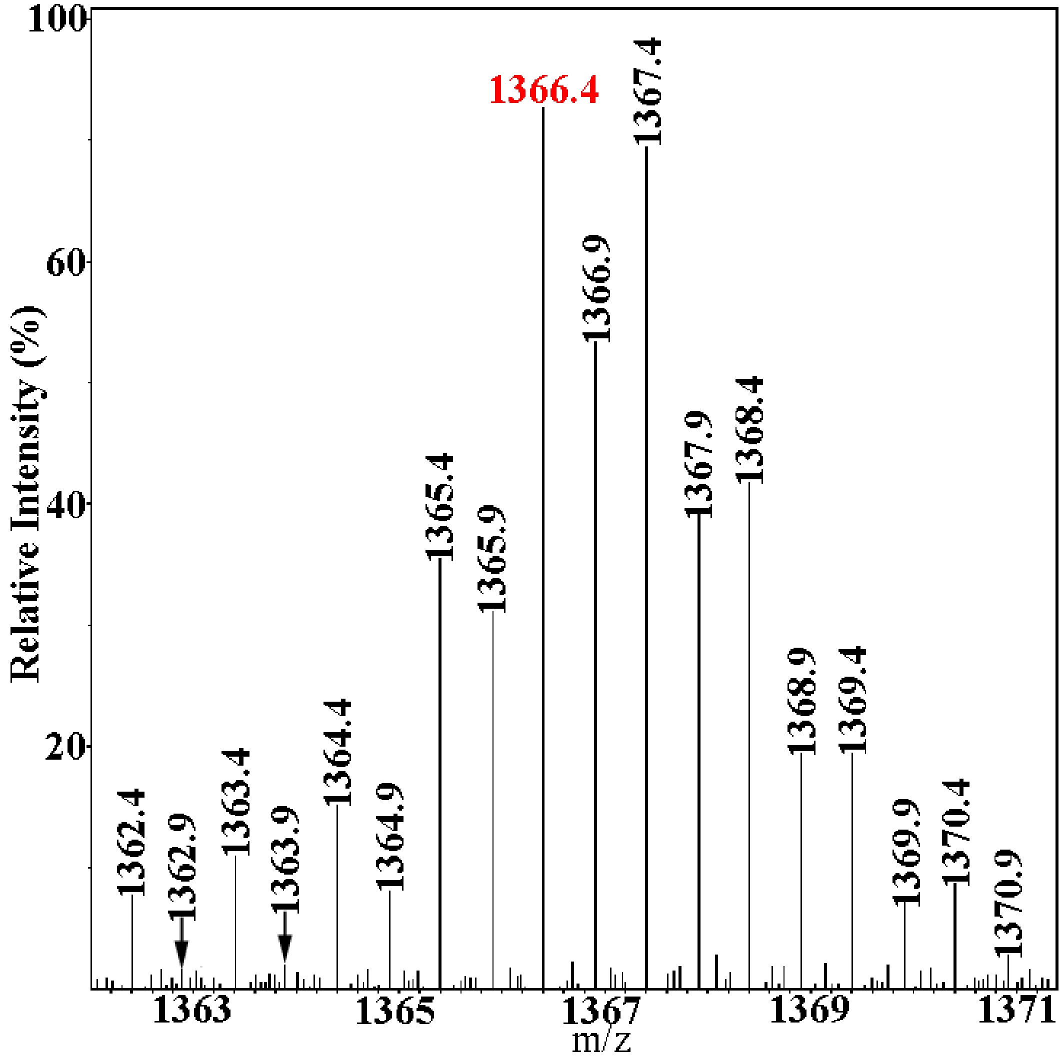

Fig. S7. Excerpt of the ESI-MS spectra of the macrocycle **2a** corresponding to [**2a** − $2NO_3^-$]$^{2+}$ fragment recorded in CH_3NO_2-CH_3CN.

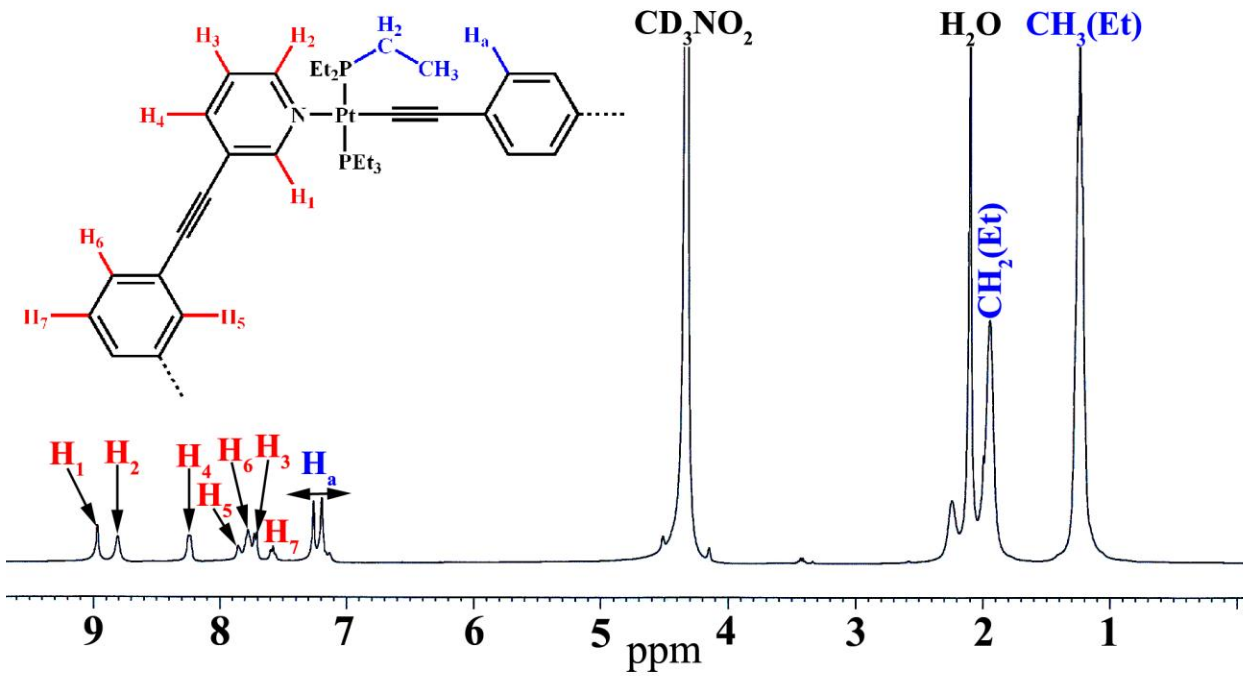

Fig. S8. [1]H NMR spectra of the macrocycle **2b** recorded in CD_3NO_2 with the peak assignments.

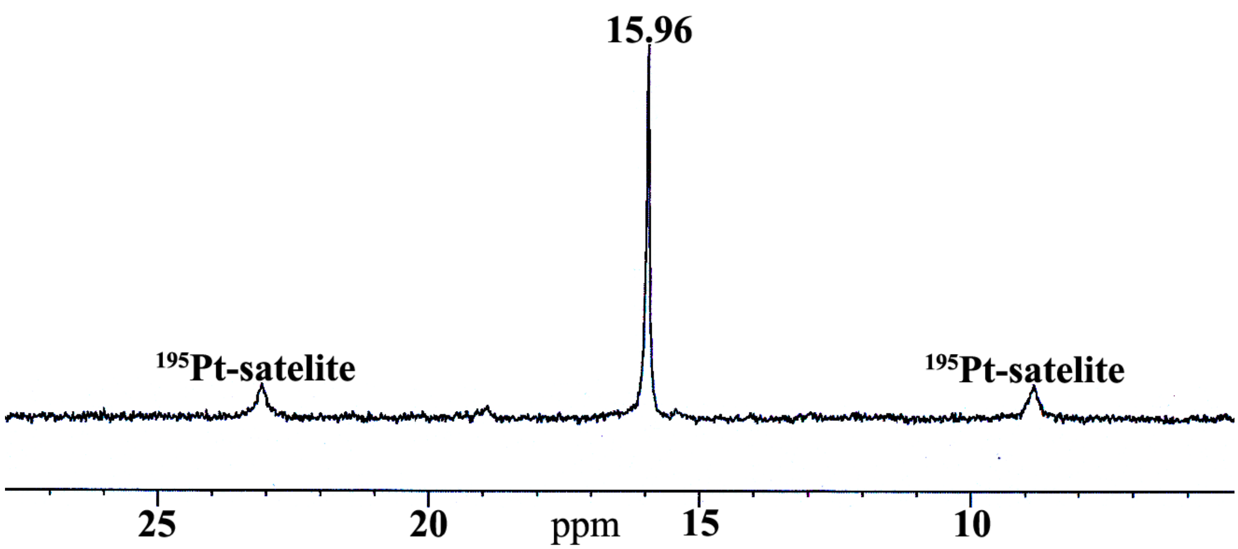

Fig. S9. [31]P NMR spectra of the macrocycle **2b** recorded in $CDCl_3$-CD_3OD solvent mixture with the peak assignments.

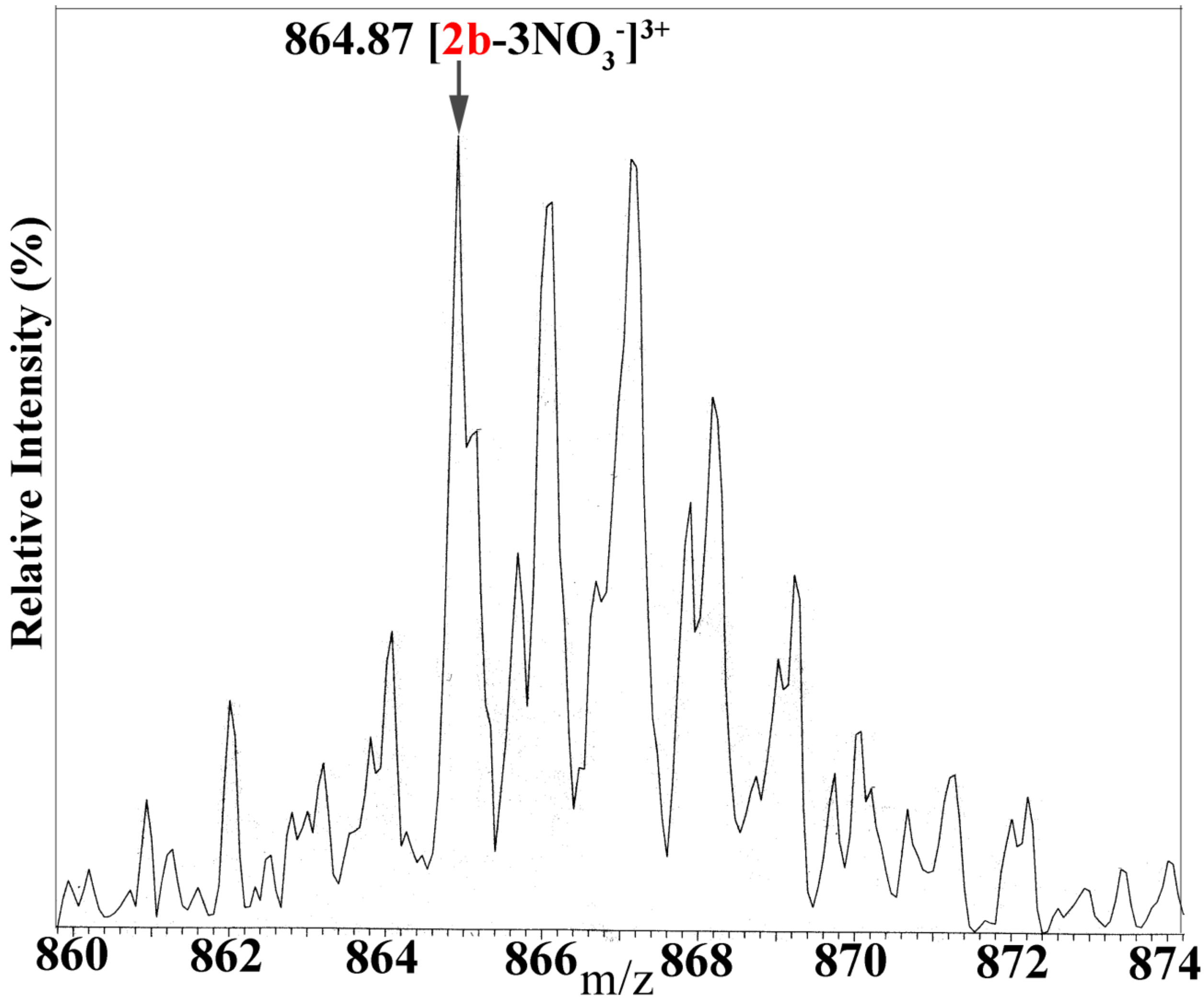

Fig. S10. Excerpt of the ESI-MS spectra of the macrocycle **2b** corresponding to [**2b** − $3NO_3^-$]$^{3+}$ fragment recorded in CH_3NO_2-CH_3CN.

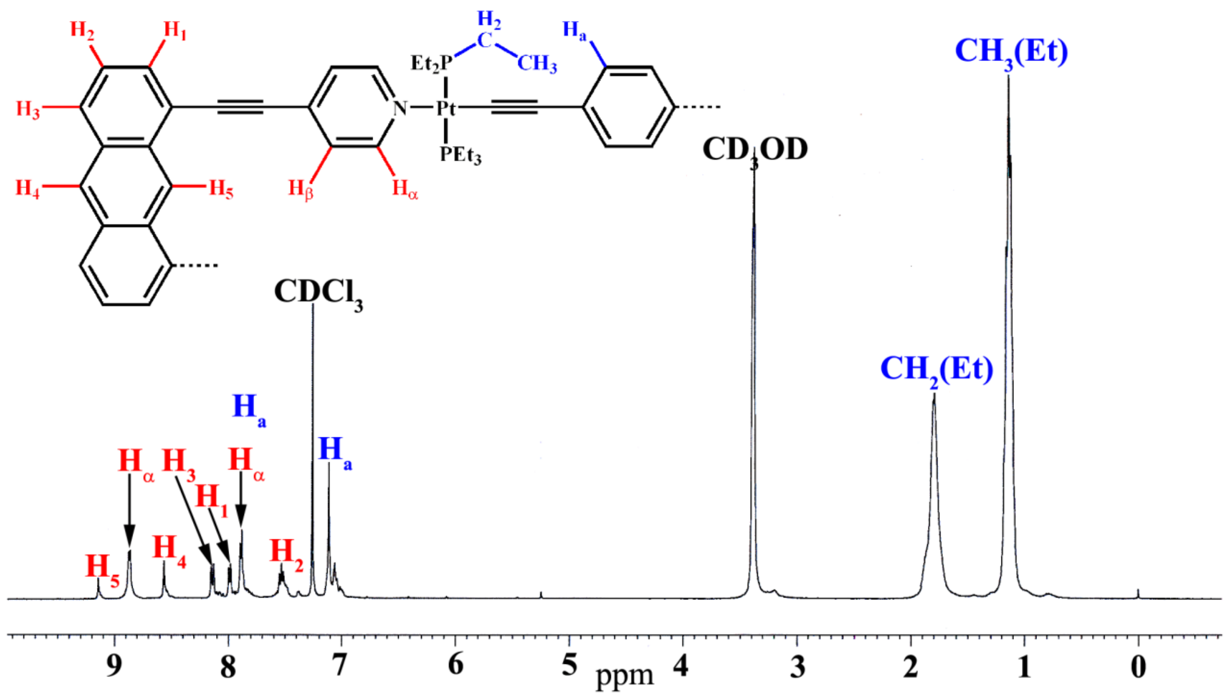

Fig. S11. [1]H NMR spectra of the macrocycle **2c** recorded in $CDCl_3$-CD_3OD solvent mixture with the peak assignments.

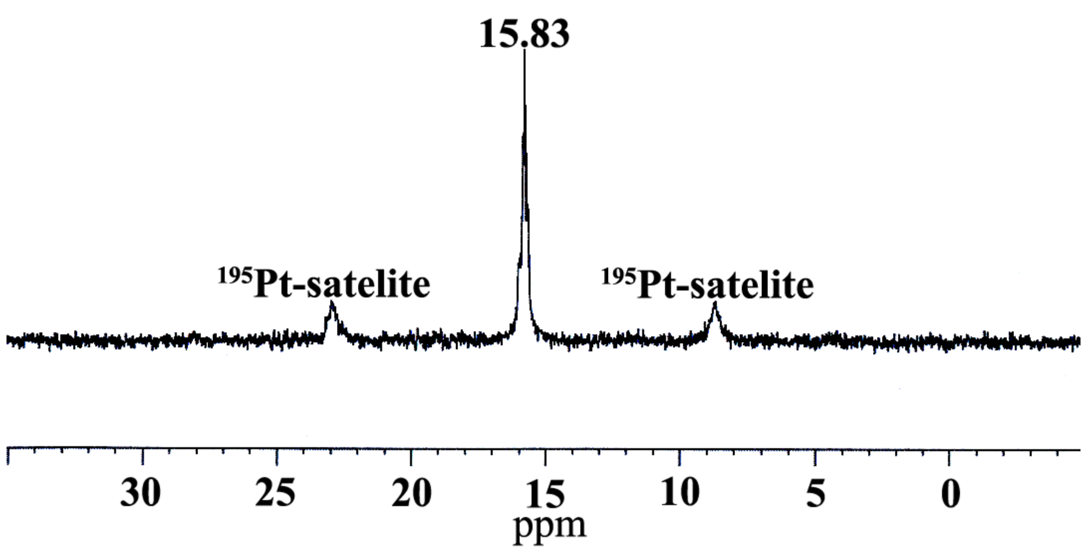

Fig. S12. [31]P NMR spectra of the macrocycle **2c** recorded in CD_3NO_2 solvent mixture with the peak assignments.

Electronic Supplementary Material (ESI) for Dalton Transactions

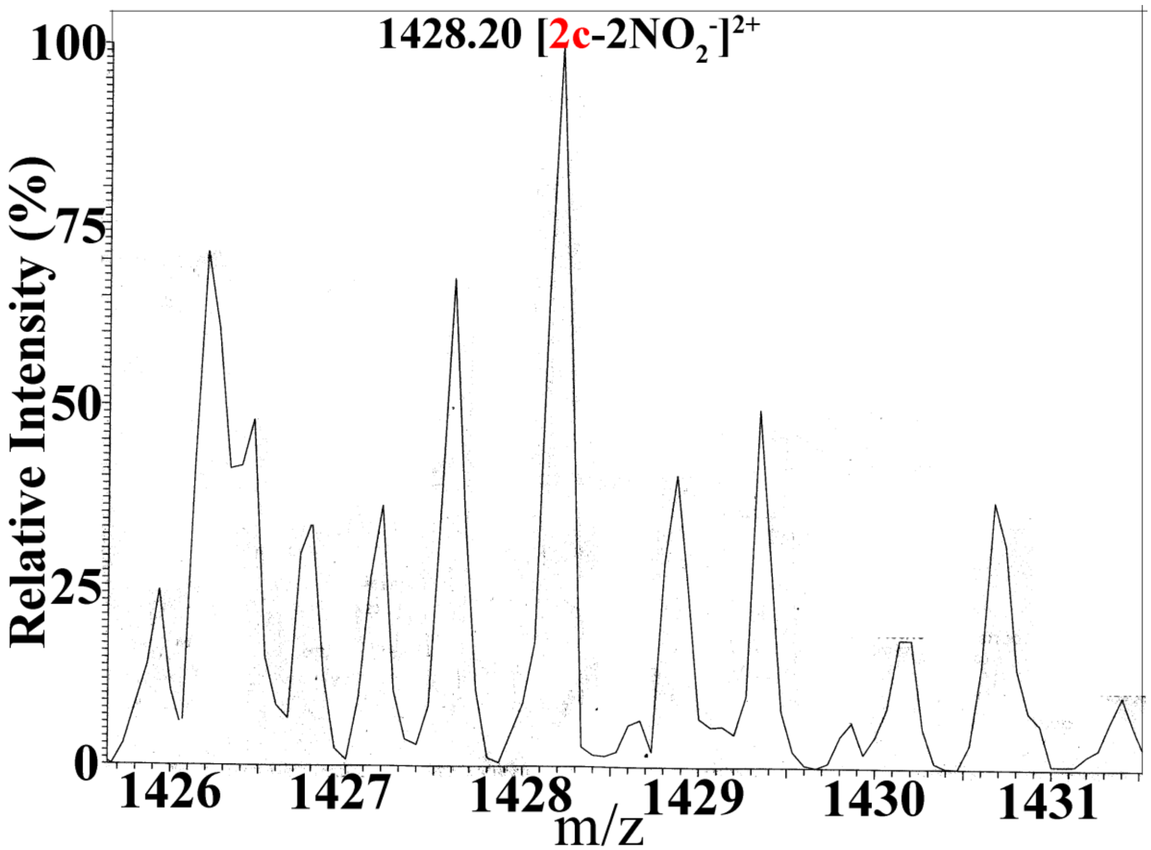

Fig. S13. Excerpts of the ESI-MS spectra of the macrocycle **2c** corresponding to [**2c** − $2NO_3^-$]$^{2+}$ fragment recorded in CH_3NO_2-CH_3CN.

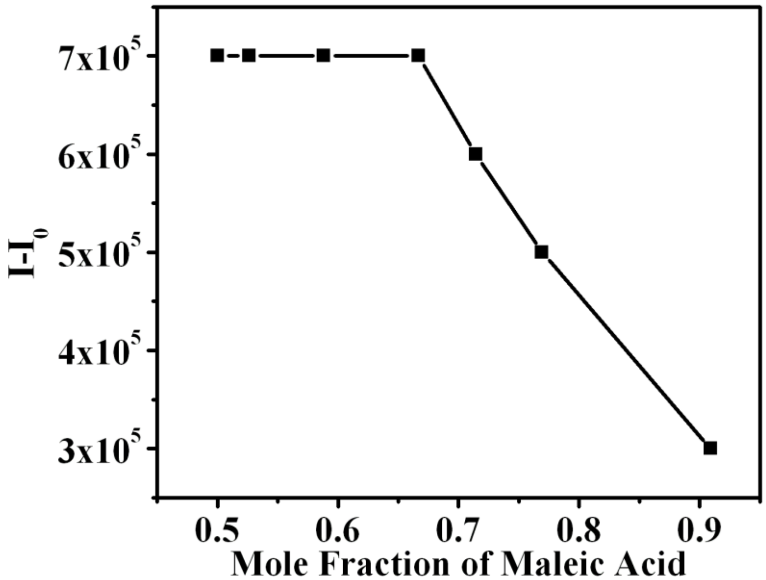

Fig. S14. Jobs plot for the fluorescence titration data of **2a** and maleic acid.

1240.71

Table S1. Crystallographic data and refinement parameters of **1a** and **2b**.

	1a	**2b**
empirical formulae	$C_{34}H_{64}I_2P_4Pt_2$	$C_{108}H_{152}N_4P_8Pt_4$
formulae weight	1240.71	2534.46
crystal system	monoclinic	monoclinic
space group	$P\ 2_1/n$	$P\ 2_1/n$
T, K	150	100
λ (Mo Kα), Å	0.71073	0.75000
a, Å	9.395(6)	17.950(4)
b, Å	13.955(9)	9.6820(19)
c, Å	17.449(11)	37.661(8)
α, °	90	90
β, °	93.387(11)	102.19(3)

γ, °	90	90
V, Å^3	2284(3)	6398(2)
Z	2	2
ρ_{calcd}, g cm^{-1}	1.804	1.316
μ, mm^{-1}	7.630	4.982
GOF[a]	1.023	1.093
R1[b] [I > 2σ(I)]	0.0817	0.0578
wR2[c] [I > 2σ(I)]	0.1782	0.1748

[a]GOF = $\{\Sigma [w(F_0^2 - F_c^2)^2]/(n - p)\}^{1/2}$, where n and p denotes the number of data points and the number of parameters, respectively. [b]R1 = $(\Sigma \, \text{II}F_0\text{I} - \text{I}F_c\text{II})/\Sigma \, \text{I}F_0\text{I}$; [c]wR2 = $\{ \Sigma [w(F_0^2 - F_c^2)^2]/\Sigma[w(F_0^2)^2]\}^{1/2}$, where $w = 1/ [\sigma^2(F_0^2) + (aP)^2 + (bP)]$ and $P = [\max (0,F_0^2) + 2F_c^2]/3$.

Table S2: Selected Bonds Distances (Å) and Angles (deg) for **1a** and **2b**.

1a

Pt(1)-C(1)	1.954(19)	Pt(1)-P(2)	2.320(6)	Pt(1)-P(1)	2.321(6)
Pt(1)-I(1)	2.6704(19)	P(1)-C(9)	1.899(15)	P(1)-C(6)	1.916(18)
P(1)-C(7B)	1.928(19)	P(1)-C(7A)	1.949(18)	P(2)-C(8T)	1.905(19)
P(2)-C(1T)	1.913(19)	P(2)-C(3T)	1.937(19)	P(2)-C(9T)	1.94(2)
P(2)-C(6T)	1.939(19)	P(2)-C(5T)	1.948(18)		

C(1)-Pt(1)-I(1)	179.7(6)	P(2)-Pt(1)-I(1)	92.22(16)
P(1)-Pt(1)-I(1)	91.22(15)	C(9)-P(1)-C(6)	105.0(13)
C(9)-P(1)-C(7B)	109.3(17)	C(6)-P(1)-C(7B)	93(2)
C(9)-P(1)-C(7A)	100.9(17)	C(6)-P(1)-C(7A)	113.6(19)

C(7B)-P(1)-C(7A)	21(2)	C(9)-P(1)-Pt(1)	115.6(8)
C(6)-P(1)-Pt(1)	112.0(11)	C(7B)-P(1)-Pt(1)	118.9(16)
C(7A)-P(1)-Pt(1)	109.4(12)	C(8T)-P(2)-C(1T)	118(2)
C(8T)-P(2)-C(3T)	38.9(19)	C(1T)-P(2)-C(3T)	106(2)
C(8T)-P(2)-C(9T)	105(3)	C(1T)-P(2)-C(9T)	40(2)
C(8T)-P(2)-Pt(1)	123.7(15)	C(1T)-P(2)-Pt(1)	117.8(15)
C(3T)-P(2)-Pt(1)	114.8(16)	C(9T)-P(2)-Pt(1)	111(2)
C(6T)-P(2)-Pt(1)	111.1(18)	C(5T)-P(2)-Pt(1)	108.7(13)

2b

Pt(1)-C(30)#1	1.96(3)	Pt(1)-N(1)	2.10(2)	Pt(1)-P(2)	2.281(8)
Pt(1)-P(1)	2.283(8)	P(1)-C(5P)	1.74(3)	P(1)-C(1P)	1.83(3)
P(1)-C(3P)	1.89(3)	Pt(2)-C(21)	1.99(3)	Pt(2)-N(2)	2.077(19)
Pt(2)-P(3)	2.291(8)	Pt(2)-P(4)	2.327(7)	P(3)-C(13P)	1.77(3)
P(3)-C(17P)	1.83(4)	P(3)-C(15P)	1.89(5)	P(3)-C(65P)	1.97(5)

C(30)#1-Pt(1)-N(1)	176.6(11)	C(30)#1-Pt(1)-P(2)	85.0(9)
N(1)-Pt(1)-P(2)	93.2(6)	C(30)#1-Pt(1)-P(1)	87.2(9)
N(1)-Pt(1)-P(1)	94.3(6)	P(2)-Pt(1)-P(1)	170.0(3)
C(5P)-P(1)-C(1P)	109.1(18)	C(5P)-P(1)-C(3P)	103.1(16)
C(1P)-P(1)-C(3P)	101.9(17)	C(5P)-P(1)-Pt(1)	113.8(13)
C(1P)-P(1)-Pt(1)	115.8(9)	C(3P)-P(1)-Pt(1)	111.7(14)
C(2P)-C(1P)-P(1)	116(2)	C(21)-Pt(2)-N(2)	179.4(9)
C(21)-Pt(2)-P(3)	89.0(8)	N(2)-Pt(2)-P(3)	91.7(5)

C(21)-Pt(2)-P(4)	88.8(8)	N(2)-Pt(2)-P(4)	90.6(5)
P(3)-Pt(2)-P(4)	176.2(4)		